Positioning Accuracy of a High-precision Planer Multi-joint Mechanism: Measurement and a Method of Link Parameter Calibration for Error Compensation

S. Fukada[1], A. Nagao[1], K. Shimizu[1]
[1]*Shinshu University, Japan*
sfukada@shinshu-u.ac.jp

Abstract

An experimental system of measuring positioning accuracy of a high-precision planer multi-joint mechanism is constructed, and measurement results are shown. To improve positioning bias error, a link parameter calibration method is discussed, and the availability of the proposed method is verified.

1 Introduction

Planer multi-joint mechanisms are used in SCARA-type manipulators, and they are in great demand on precision assembly lines because they have a wide work range but a small setting area. However, the positioning accuracy of current multi-joint manipulators is not high: They often have positioning errors over 100 s microns. The positioning errors can be divided into bias errors and repeatability errors, and it is possible to compensate for the bias error with appropriate calibration methods. In our previous report, a novel arrangement for high-precision driving mechanism was proposed to improve the positioning repeatability of the current SCARA-type manipulator, and an experimental model was developed. In this report, a new method of measuring positioning accuracy of the planer multi-joint mechanism is proposed.

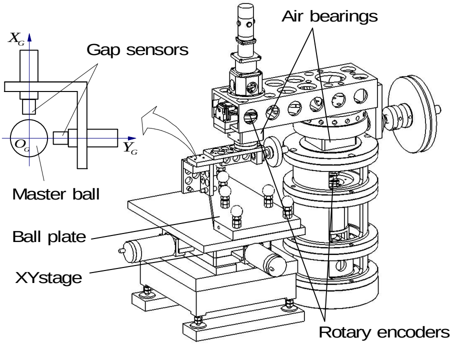

Figure 1: Experimental apparatus

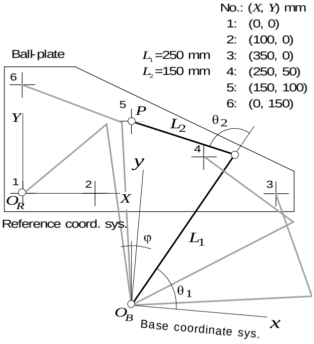

Figure 2: Ball-plate and arm poses

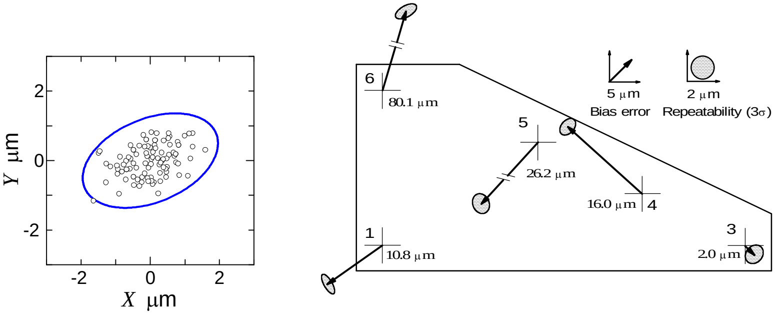

(a) Repeatability (N=100) (b) Bias error and repeatability at 5 positions (N=30)

Figure 3: Measurement result of positioning repeatability and accuracy

A link parameter calibration method is also proposed based on the measured positioning error, and the availability of the method is verified experimentally.

2 Experimental apparatus

Figure 1 shows the experimental positioning mechanism with measurement system. The experimental apparatus is a high-precision planer multi-joint positioning system with two joints: It was constructed in the previous report by applying the drive mechanism proposed. High precision air bearings and friction drive mechanisms are adopted, and the joint angles are controlled with feedback signals from actual joint angles detected by rotary encoders with ultra-high-resolution of 720×10^4 ppr.

A measurement system is constructed by using master balls and non-contact gap sensors. First, the master steel balls (diameter of 28.575 mm) are set on the workspace plane, and two gap sensors are attached to the positioning mechanism at the end of the manipulator arm in X_G and Y_G directions. The arm is positioned to the master ball, and the positioning error can then be measured by reading the gap sensors with coordinate transformation. To measure positioning bias error, a master ball-plate with six balls is constructed. Figure 2 shows the coordinates of the balls and the arm posing while approaching the balls. In the following experiments, all balls except ball No. 2 are used: The actual positions of the balls on the reference coordinate system X-Y of the ball-plate were measured by a CMM for calibration.

3 Measurement results

Figure 3(a) shows that 100 times positioning repeatability at a target point of base coordinates $(x, y) = (0, 300)$ mm. The ellipse is an envelope of $\pm 3\sigma$ determined by a variance-covariance matrix: It shows precision positioning repeatability with dispersion error of less than ±2 microns. (b) shows bias errors and repeatability at five positions: It shows that an extreme bias error of more than 80 microns remained.

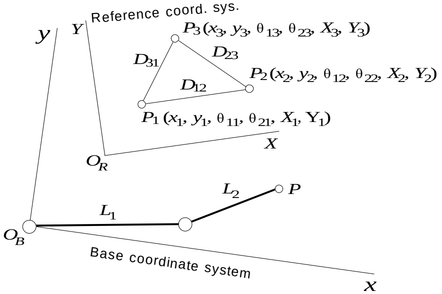

Figure 4: principle of link length calibration

4 Link parameter calibration

To improve the accuracy of the positioning system, an accurate method of link parameter calibration is here proposed. Figure 4 shows the three positions of arbitrary points P_m (m=1, 2, 3) selected from among five reference positions on the ball-plate. Two points are extracted from these three points, and their norms are squared as follows:

$$\left\|\mathbf{x}_1 - \mathbf{x}_2\right\|^2 = {D_{12}}^2, \quad \left\|\mathbf{x}_2 - \mathbf{x}_3\right\|^2 = {D_{23}}^2, \quad \left\|\mathbf{x}_3 - \mathbf{x}_1\right\|^2 = {D_{31}}^2 \tag{1}$$

where $\mathbf{x}_m=(x_m, y_m)$ is the base coordinates given by the following equation.

$$\left.\begin{aligned} x &= L_1 \cos\theta_1 + L_2 \cos(\theta_1 + \theta_2) \\ y &= L_1 \sin\theta_1 + L_2 \sin(\theta_1 + \theta_2) \end{aligned}\right\} \tag{2}$$

Substituting eq. (2) into eq. (1), L_1 and L_2 are derived by the following equations:

$$\left.\begin{aligned} L_1 &= \sqrt{p_{12}{D_{12}}^2 - p_{23}{D_{23}}^2 + p_{31}{D_{31}}^2} \\ L_2 &= \sqrt{-q_{12}{D_{12}}^2 + q_{23}{D_{23}}^2 + q_{31}{D_{31}}^2} \end{aligned}\right\} \tag{3}$$

$$\left.\begin{aligned} &p_{12} = S_{31}\left(S_{31}T_{23} - S_{23}T_{31}\right)/A, \quad q_{12} = S_{31}\left(R_{23}S_{31} - R_{31}S_{23}\right)/A \\ &p_{23} = S_{31}\left(S_{31}T_{12} - S_{12}T_{31}\right)/A, \quad q_{23} = S_{31}\left(R_{12}S_{31} - R_{31}S_{12}\right)/A \\ &p_{31} = \left(S_{23}S_{31}T_{12} - S_{12}S_{31}T_{23}\right)/A, \, q_{31} = \left(R_{23}S_{12}S_{31} - R_{12}S_{23}S_{31}\right)/A \\ &A = \left(R_{12}S_{31} - R_{31}S_{12}\right)\left(S_{31}T_{23} - S_{23}T_{31}\right) - \left(R_{23}S_{31} - R_{31}S_{23}\right)\left(S_{31}T_{12} - S_{12}T_{31}\right) \end{aligned}\right\} \tag{4}$$

$$\left.\begin{aligned} R_{vw} &= \left(\cos\theta_{1v} - \cos\theta_{1w}\right)^2 + \left(\sin\theta_{1v} - \sin\theta_{1w}\right)^2 \\ S_{vw} &= \left(\cos\theta_{1v} - \cos\theta_{1w}\right)\left\{\cos(\theta_{1v} + \theta_{2v}) - \cos(\theta_{1w} + \theta_{2w})\right\} \\ &\quad + \left(\sin\theta_{1v} - \sin\theta_{1w}\right)\left\{\sin(\theta_{1v} + \theta_{2v}) - \sin(\theta_{1w} + \theta_{2w})\right\} \\ T_{vw} &= \left\{\cos(\theta_{1v} + \theta_{2v}) - \cos(\theta_{1w} + \theta_{2w})\right\}^2 + \left\{\sin(\theta_{1v} + \theta_{2v}) - \sin(\theta_{1w} + \theta_{2w})\right\}^2 \end{aligned}\right\} \tag{5}$$

Here, D_{12}, D_{23} and D_{31} in eq. (1) are determined from measured bias errors of figure 3(b), and θ_1 and θ_2 in eq. (2) can be known from the controlled joint angles. This method can simply calibrate only the link lengths from positioning errors of three arbitrarily selected points: The compensation of link parameters is then completed based on all the combinations by choosing three points from among five positions on the ball-plate. The measurement of positioning error is re-examined using the compensated link parameters, and link lengths are calibrated again using the newly obtained measurement result, and the link parameters are revised. These cycles of link-parameter-compensation and measurement are repeated for several steps, and the accuracy improvement is evaluated. Figure 5 shows measurement result of the positioning error after the final compensation step No. 4. Figure 6 shows transition of RMS value of the positioning bias error for the five positions and the link length nominal values in each of the steps. The link parameters are calibrated by the proposed method, and the accuracy of the positioning mechanism is found to be improved: a maximum bias error of less than 9 microns, and RMS value of less than 5 microns. The availability of the proposed method is thus verified, and the superior accuracy of the developed positioning mechanism is demonstrated.

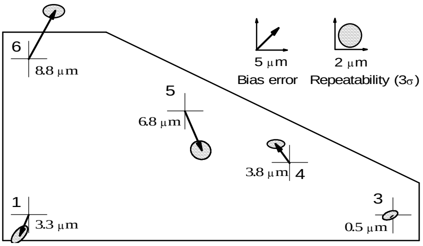

Figure 5: Positioning error after link length calibration

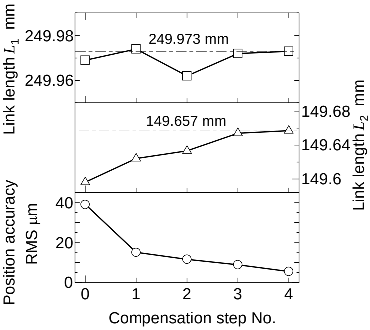

Figure 6: Transition of link lengths and positioning accuracy

5 Conclusion

A measurement system for positioning accuracy of the high-precision planer multi-joint mechanism is created using master ball-plate and non-contact gap sensors. By using this measurement system and the proposed link parameter calibration method, a high-precision planer multi-joint mechanism with bias error less than 5 microns (RMS) and dispersion error less than ±2 microns (±3σ) is realized.

References:

[1] S. Fukada, Y. Yanagihara: Proc. 7th euspen Int. Conf. (2007) p. 172-175.
[2] S. Fukada: Int. J. Automation Technology, Vol. 3, No. 3 (2009) p. 319-333.